

# Controllability Analysis for Current Profile Control in Tokamaks

Yongsheng Ou and Eugenio Schuster

**Abstract**—The control of the toroidal current density spatial profile in tokamak plasmas will be absolutely critical in future commercial-grade reactors to enable high fusion gain, noninductive sustainment of the plasma current for steady-state operation, and magnetohydrodynamic (MHD) instability-free performance. Since the actuators that are available to achieve a predefined desired current profile are constrained by physical limitations, experiments have shown that some target profiles may not be achievable for all arbitrary initial conditions. This clearly defines a controllability problem, where the transport dynamics of the toroidal current density is governed by a parabolic partial differential equation with diffusivity-interior-boundary actuation. We first prove that the system is not completely controllable and later provide an estimate of the unreachable region.

## I. INTRODUCTION

Fusion is the process by which the sun produces heat and sunlight. If we can make this process generate energy on Earth, it will represent a clean and unlimited energy source. As nuclei have positive charges, they repel each other when they try to fuse together. To overcome the Coulomb force, the temperatures of the reactants have to be increased to an extremely high level (50 to 200 million Kelvin). At such high temperatures, the hydrogen gas ionizes and becomes a plasma. The major challenge in fusion is the confinement of the plasma, where nuclear fusion reactions take place.

One of the most promising magnetic-confinement devices is the tokamak. Tokamaks bend magnetic field lines into a torus structure. Charged particles can be confined because they follow the generated magnetic field lines. Toroidal field coils and poloidal field coils (See Fig. 1) form helicoidal endless magnetic field lines trapping the ionized particles within the torus structure. The magnetic fields produce an external force (magnetic pressure), which balance the internal pressure (kinetic pressure) created by the hot gas. It is possible to use the poloidal component of the helicoidal magnetic lines to define nested toroidal surfaces corresponding to constant values of the poloidal magnetic flux. The poloidal flux  $\psi$  at a point  $P$  in the  $(r, z)$  cross section of the plasma (i.e., poloidal cross section) is the total flux through the surface  $S$  bounded by the toroidal ring passing through  $P$ , i.e.,  $\psi = \frac{1}{2\pi} \int B_{pol} dS$ . Thus, the poloidal flux  $\psi$  can be used as a spatial coordinate.

The development of current profile controllers in present experimental tokamaks is aimed at saving long trial-and-error periods of time currently spent by fusion experimentalists

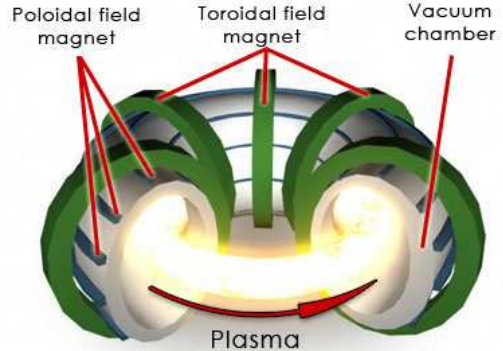


Fig. 1. Scheme of a tokamak device. The toroidal field (TF) coils are wrapped “poloidally” around the torus (the short way, going through the center hole), while the poloidal field (PF) coils are wrapped “toroidally” (the long way) around the torus. Current flowing in these conducting coils produces the helicoidal magnetic field that confines the plasma. The plasma contained within the device can be represented by a set of nested contours of constant poloidal magnetic flux.

trying to manually adjust the time evolutions of the actuators to achieve a desired current profile. The evolution in time of the current profile is related to the evolution of the poloidal magnetic flux, which is modeled in normalized cylindrical coordinates using a partial differential equation (PDE) usually referred to as the magnetic diffusion equation. Since the actuators that are used to achieve the desired target profiles are constrained, experiments have shown that some of the target profiles may not be achievable for all arbitrary initial conditions. Therefore, given an initial current profile, it is desirable to identify in advance those unreachable target profiles in order to prevent experimentalists from wasting enormous amounts of effort and time attempting to achieve them. From the perspective of control, this is clearly a controllability issue.

Controllability is a fundamental concept in modern control theory and there are numerous degrees of state and output controllability that are formally defined in the literature [1], [2]. As for the controllability of PDE systems, prior work includes [3], [4], [5]. Using the Hilbert Uniqueness method, Liu and Williams [3] investigate the problem of exact controllability through Neumann boundary conditions for the wave equation and prove that the system is exactly controllable. In [4], Bezerra and Menezes prove the approximate controllability of a semilinear heat equation, when the nonlinear term is globally Lipschitz and depends on both the state  $x$  and its spatial gradient  $\nabla x$ . In [5], Lin and his colleagues discuss the controllability of a nonlinear degenerate parabolic systems with bilinear control. Based on the shrinking property of the solutions, they prove that the system is not globally approximately controllable, give

This work was supported in part by a grant from the NSF CAREER award program (ECCS-0645086).

Y. Ou (yoo205@lehigh.edu), and E. Schuster are with the Department of Mechanical Engineering and Mechanics, Lehigh University, Bethlehem, PA 18015, USA.

an approximate null controllability result, and finally prove that the system is not globally exactly null controllable. The requirements of our problem imply that the system must be completely controllable. Formally, a system is said to be *completely controllable* [6] if it can be driven from any initial state  $x_0$  to an arbitrary finite terminal state  $x_f$  with an admissible control.

This paper is organized as follows. In Section II, an infinite-dimensional dynamic model for the evolution of the poloidal magnetic flux is introduced. The control problem is stated in Section III. In Section IV, we provide the functional setting and necessary technical lemmas that will be used in this paper. In Section V, we study the controllability of a class of systems. The results are used in Section VI to demonstrate that the current profile system is not completely controllable and to show the existence of an unreachable region. In Section VII, an estimate of the unreachable region is provided based on data from the DIII-D tokamak. Finally, we close the paper by stating the conclusions and future research issues in Section VIII.

## II. CURRENT PROFILE EVOLUTION MODEL

Let  $\rho$  be an arbitrary coordinate indexing the magnetic surface. Any quantity constant on each magnetic surface could be chosen as the variable  $\rho$ . We choose the mean geometric radius of the magnetic surface as the variable  $\rho$ , i.e.,  $\pi B_{\phi,o} \rho^2 = \Phi$ , where  $\Phi$  is the toroidal magnetic flux and  $B_{\phi,o}$  is the reference toroidal magnetic field at  $R_o$  ( $R_o$  can be the geometric center of the plasma  $R_{geo}$ ). The evolution of the poloidal flux in normalized cylindrical coordinates is given by the magnetic diffusion equation [7],

$$\frac{\partial \psi}{\partial t} = \frac{\eta(T_e)}{\mu_o \rho_b^2 \hat{F}^2 \hat{\rho}} \frac{\partial}{\partial \hat{\rho}} \left( \hat{F} \hat{G} \hat{H} \frac{\partial \psi}{\partial \hat{\rho}} \right) - R_o \hat{H} \eta(T_e) \frac{\langle \bar{j}_{NI} \cdot \bar{B} \rangle}{B_{\phi,o}}, \quad (1)$$

where  $\eta(T_e)$  denotes the plasma resistivity,  $T_e$  is the electron temperature,  $\mu_o = 4\pi \times 10^{-7} \text{ (H/m)}$  represents the vacuum permeability,  $\hat{\rho} = \frac{\rho}{\rho_b}$  denotes the normalized space coordinate ( $\rho_b$  is the radius of last closed flux surface),  $\hat{F}, \hat{G}, \hat{H}$  are  $\hat{\rho}$ -dependent geometric factors [7],  $\bar{B}$  is the toroidal magnetic field,  $\bar{j}_{NI}$  denotes the non-inductive source of current density (neutral beam, electron cyclotron, etc.), and  $\langle \rangle$  represents the average value on a magnetic surface.

We consider  $\bar{n}(t)$ ,  $I(t)$ , and  $P_{tot}(t)$  as the physical actuators of the system, where  $I(t)$ ,  $\bar{n}(t)$  and  $P_{tot}(t)$  represent the total plasma current, the line average density and the total power of the non-inductive current drives, respectively. The boundary conditions of (1) are given by

$$\left. \frac{\partial \psi}{\partial \hat{\rho}} \right|_{\hat{\rho}=0} = 0, \quad \left. \frac{\partial \psi}{\partial \hat{\rho}} \right|_{\hat{\rho}=1} = \frac{\mu_o}{2\pi} \frac{R_o}{\hat{G}|_{\hat{\rho}=1} \hat{H}|_{\hat{\rho}=1}} I(t). \quad (2)$$

During ‘‘Phase I’’ (see Fig. 2), mainly governed by the ramp-up phase, the plasma current is mostly driven by induction. In this case, it is possible to decouple the equation for the evolution of the poloidal flux from the evolution equations for the temperature  $T_e(\hat{\rho}, t)$  and the density  $n_e(\hat{\rho}, t)$ . Highly simplified models for the temperature and non-inductive toroidal current density are chosen for this phase.

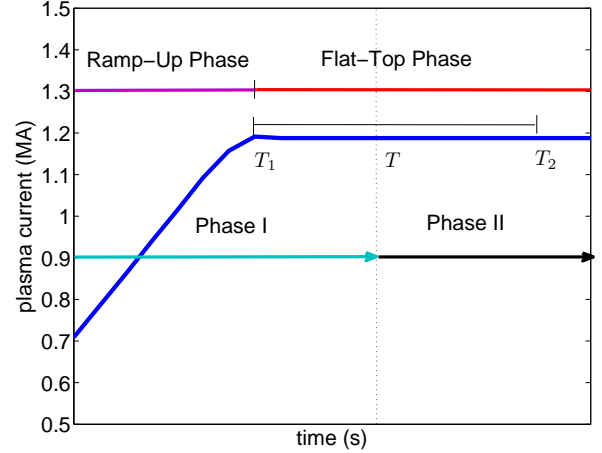


Fig. 2. The control problem focuses on phase I that includes the ramp-up phase and the first part of the flat-top phase. The control goal is to drive during the ramp-up phase the magnetic flux profile from some initial arbitrary condition to a predefined target profile at some time  $T$  between the time window  $[T_1, T_2]$ .

The profiles are assumed to remain fixed. The responses to the actuators are simply scalar multiples of the reference profiles. These reference profiles are taken from a DIII-D tokamak discharge [7].

The temperature  $T_e$  is assumed proportional to  $\frac{I(t)\sqrt{P_{tot}}}{\bar{n}(t)}$ , and can be written as

$$T_e(\hat{\rho}, t) = k_{Te} T_e^{profile}(\hat{\rho}) \frac{I(t)\sqrt{P_{tot}}}{\bar{n}(t)}, \quad (3)$$

where  $T_e^{profile}$  has been identified from DIII-D and is given in [7], and  $k_{Te} = 1.7295 \cdot 10^{10} \text{ m}^{-3} \text{ A}^{-1} \text{ W}^{-1/2}$ .

The non-inductive toroidal current density  $\frac{\langle \bar{j}_{NI} \cdot \bar{B} \rangle}{B_{\phi,o}}$  is assumed proportional to  $\frac{I(t)^{1/2} P_{tot}(t)^{5/4}}{\bar{n}(t)^{3/2}}$ , and can be written as

$$\frac{\langle \bar{j}_{NI} \cdot \bar{B} \rangle}{B_{\phi,o}} = k_{NIpar} j_{NIpar}^{profile}(\hat{\rho}) \frac{I(t)^{1/2} P_{tot}(t)^{5/4}}{\bar{n}(t)^{3/2}}, \quad (4)$$

where  $j_{NIpar}^{profile}$  has been identified from DIII-D and is given in [7], and  $k_{NIpar} = 1.2139 \cdot 10^{18} \text{ m}^{-9/2} \text{ A}^{-1/2} \text{ W}^{-5/4}$ .

The resistivity  $\eta$  scales with the temperature  $T_e$  as

$$\eta(\hat{\rho}, t) = \frac{k_{eff} Z_{eff}}{T_e^{3/2}(\hat{\rho}, t)}, \quad (5)$$

where  $Z_{eff} = 1.5$ , and  $k_{eff} = 4.2702 \cdot 10^{-8} \text{ } \Omega \text{ m (keV)}^{3/2}$ .

## III. CONTROL PROBLEM DESCRIPTION

The safety factor  $q$  profile depends on the current profile (and vice versa). Thus, many physicists speak interchangeably of the current profile and the  $q$ -profile. Another quantity related to  $q$  is its inverse, known as the rotational transform  $\iota(\psi) = 1/q(\psi)$ . It can be shown that  $\iota(\psi)$  is proportional to the total current inside the flux surface represented by the poloidal flux value  $\psi$ . The safety factor  $q$  and the rotational transform  $\iota$  are related and defined as

$$\iota(\rho, t) = \frac{1}{q(\rho, t)} = \frac{\partial \psi(\rho, t)}{\partial \Phi}. \quad (6)$$

The constant relationship between  $\Phi$  and  $\rho$ ,  $\rho = \sqrt{\frac{\Phi}{\pi B_{\phi,o}}}$ , and the definition of the normalized radius allow us to rewrite (6) as

$$i(\hat{\rho}, t) = \frac{\partial \psi}{\partial \hat{\rho}} \frac{1}{B_{\phi,o} \rho_b^2 \hat{\rho}}. \quad (7)$$

The control objective, as well as the dynamic models for current profile evolution, depend on the phases of the discharge (Fig. 2). During ‘‘Phase I,’’ which is the focus of this work, the control goal is to drive the current profile from any arbitrary initial condition to a prescribed target or desirable profile at some time  $T \in (T_1, T_2)$  in the flat-top phase of the total current  $I(t)$  evolution. ‘‘Phase I’’ can be divided into two parts, the ramp-up phase and the early stage of flattop phase. During ‘‘Phase I’’, the three actuators  $I(t)$ ,  $\bar{n}(t)$  and  $P_{tot}(t)$  are assumed available for current profile control. The physical ranges for  $I(t)$ ,  $\bar{n}(t)$  and  $P_{tot}(t)$  are given by

$$\begin{cases} 0 \leq I(t) \leq I_{max} \\ |dI(t)/dt| \leq dI_{max}, \end{cases} \quad (8)$$

$$I(\text{MA}) \leq \bar{n}(t) \times 10^{-13} \leq 5I(\text{MA}), \quad (9)$$

$$0 < P_{min} \leq P_{tot}(t) \leq P_{max}. \quad (10)$$

The lower and upper limits for the line average density in (9) are set to prevent density instabilities and disruptions. The upper limit is approximately half of the Greenwald limit [8]. To accurately reproduce experimental discharges, we must add constraints for  $I(t)$  at the initial time of ‘‘Phase I’’, i.e.,

$$I(t = 0s) = I_0. \quad (11)$$

It is worth to note that we can rewrite the equation for the evolution of the poloidal flux (1) as

$$\frac{\partial \psi}{\partial t} = f_1(\hat{\rho})w(t) \frac{\partial}{\partial \hat{\rho}} \left( f_4(\hat{\rho}) \frac{\partial \psi}{\partial \hat{\rho}} \right) + f_2(\hat{\rho})u(t) \quad (12)$$

with boundary conditions

$$\frac{\partial \psi}{\partial \hat{\rho}} \Big|_{\hat{\rho}=0} = 0, \quad \frac{\partial \psi}{\partial \hat{\rho}} \Big|_{\hat{\rho}=1} = v(t), \quad (13)$$

and initial condition

$$\psi(\hat{\rho}, 0) = \psi_0(\hat{\rho}), \quad (14)$$

where

$$f_1(\hat{\rho}) = \frac{k_{eff} Z_{eff}}{k_{Te}^{3/2} \mu_o \rho_b^2 \hat{\rho}} \frac{1}{\hat{F}^2(\hat{\rho}) (T_e^{profile}(\hat{\rho}))^{3/2}}, \quad (15)$$

$$w(t) = \left( \frac{\bar{n}(t)}{I(t) \sqrt{P_{tot}}} \right)^{3/2}, \quad (16)$$

$$f_2(\hat{\rho}) = -R_o \hat{H} \mu_o \rho_b^2 \hat{F}^2(\hat{\rho}) k_{N1par} j_{N1par}^{profile}(\hat{\rho}) f_1(\hat{\rho}), \quad (17)$$

$$u(t) = \frac{\sqrt{P_{tot}(t)}}{I(t)}, \quad (18)$$

$$k_3 = \frac{\mu_o R_o}{2\pi \hat{G}|_{\hat{\rho}=1} \hat{H}|_{\hat{\rho}=1}}, \quad (19)$$

$$v(t) = k_3 I(t), \quad (20)$$

$$f_4(\hat{\rho}) = \hat{F} \hat{G} \hat{H}. \quad (21)$$

In the PDE system (12)-(13),  $u(t)$  is the interior control,  $v(t)$  is the boundary control and  $w(t)$  is the diffusivity control, which satisfy the following constraints,

$$\begin{aligned} \mathcal{U} &= \{u(t) \mid 0 < u_{min} \leq u(t) \leq u_{max}, u \in C^1[0, T]\}, \\ \mathcal{V} &= \{v(t) \mid 0 < v_{min} \leq v(t) \leq v_{max}, v \in C^1[0, T]\}, \\ \mathcal{W} &= \{w(t) \mid 0 < w_{min} \leq w(t) \leq w_{max}, w \in C^1[0, T]\}. \end{aligned} \quad (22)$$

#### IV. PRELIMINARIES

We define the following functional space

$$L^2(\Omega) = \left\{ f(x) \mid \int_{\Omega} f^2(x) dx < \infty \right\}. \quad (23)$$

*Lemma 1 (Young’s inequality):* Given functions  $\tilde{f}, \tilde{g} \in L^2(0, 1)$  and  $\mu > 0$  ( $\mu \in \mathbb{R}$ ), then we have the following inequality,

$$\int_0^1 \tilde{f} \tilde{g} dx \leq \frac{1}{2\mu} \int_0^1 \tilde{f}^2 dx + \frac{\mu}{2} \int_0^1 \tilde{g}^2 dx. \quad (24)$$

*Lemma 2 (Dirichlet Poincare’ inequality):* Let  $U$  be a bounded, connected, open subset of  $\mathbb{R}^n$ , and  $\tilde{f}$  be a  $C^1$  function, with  $\tilde{f} = 0$  on the boundary  $\partial U$ . Then, there exists a positive constant  $C$ , depending only on  $n$  and  $U$ , such that

$$\int_U \tilde{f}^2 dx \leq C \int_U (\nabla \tilde{f})^2 dx. \quad (25)$$

We present in the appendix a proof of this lemma.

*Lemma 3 (Green’ formulas [9]):* Let  $U = (0, 1)$ . Given functions  $\hat{f}, \hat{g} \in C^2[0, 1]$ ,

$$\int_0^1 \hat{f} \frac{d^2 \hat{g}}{dx^2} dx = - \int_0^1 \frac{d\hat{f}}{dx} \frac{d\hat{g}}{dx} dx + \hat{f} \frac{d\hat{g}}{dx} \Big|_0^1. \quad (26)$$

#### V. A PRIORI THEOREM

Before tackling the controllability properties of the current profile control problem, we first study a more general class of control problems. Consider a 1-D parabolic PDE over

$$\Omega_T = \{(x, t) \mid x \in \Omega = [0, 1]; 0 \leq t \leq T\},$$

which is governed by

$$\frac{\partial \phi}{\partial t} = f_1(x)w(t) \frac{\partial}{\partial x} \left( f_4(x) \frac{\partial \phi}{\partial x} \right) + \sum_{i=1}^3 g_i(x)u_i(t), \quad (27)$$

with boundary conditions

$$\frac{\partial \phi}{\partial x} \Big|_{x=0} = 0, \quad \frac{\partial \phi}{\partial x} \Big|_{x=1} = 0, \quad (28)$$

and initial condition

$$\phi_0(x) = \phi(x, 0), \quad (29)$$

where  $f_1(x) > 0$ ,  $f_4(x) > 0$  and  $g_i(x) \in L^2(\Omega)$  ( $i = 1, 2, 3$ ) are coefficients, dependent on the spatial coordinate  $x$  but not on the time coordinate  $t$ , that satisfy

$$\begin{cases} 0 < f_{1min} \leq f_1(x) \\ 0 < f_{4min} \leq f_4(x), \end{cases} \quad (30)$$

and

$$\int_0^1 g_i^2(x)dx = G_i, \quad i = 1, 2, 3. \quad (31)$$

The control inputs  $w(t)$  and  $u_i(t) > 0$  are constrained to the spaces  $\mathcal{W}$  and  $\mathcal{U}$  respectively, i.e.,

$$w(t) \in \mathcal{W}, \quad u_i(t) \in \mathcal{U}, \quad i = 1, 2, 3. \quad (32)$$

Let us define

$$\theta(x, t) = \sqrt{f_4(x)} \frac{\partial \phi}{\partial x}. \quad (33)$$

The control objective is to drive  $\theta(x, t)$  from an arbitrary initial condition  $\theta(x, 0)$  to a desired profile  $\theta^{des}$ , using feasible control inputs  $w(t)$  and  $u_i(t)$  ( $i = 1, 2, 3$ ).

*Theorem 4:* Assume  $\theta(x, 0) \in C^0(\Omega) \cap L^2(\Omega)$ , then the system defined by (27)-(33) is not completely controllable in  $\Omega_T$ .

*Proof:* First, we consider a positive-definite quadratic form  $V(\theta)$  defined as

$$V(\theta) = \frac{1}{2} \|\theta(x, t)\|^2 = \frac{1}{2} \int_0^1 \left( \sqrt{f_4(x)} \frac{\partial \phi}{\partial x} \right)^2 dx. \quad (34)$$

Then, we compute the time derivative of  $V$ ,

$$\dot{V}(\theta) = \int_0^1 f_4(x) \frac{\partial \phi}{\partial x} \frac{\partial^2 \phi}{\partial x \partial t} dx. \quad (35)$$

By defining  $\hat{f} = f_4(x) \frac{\partial \phi}{\partial x}$  and  $\hat{g} = \int \frac{\partial \phi}{\partial t} dx$ , we can apply *Lemma 3 (Green' formulas)* to (35) to obtain

$$\begin{aligned} \dot{V}(\theta) &= - \int_0^1 \frac{\partial}{\partial x} \left( f_4(x) \frac{\partial \phi}{\partial x} \right) \frac{\partial \phi}{\partial t} dx + f_4(x) \frac{\partial \phi}{\partial t} \frac{\partial \phi}{\partial x} \Big|_0^1 \\ &= - \int_0^1 \frac{\partial}{\partial x} \left( f_4(x) \frac{\partial \phi}{\partial x} \right) \frac{\partial \phi}{\partial t} dx. \end{aligned} \quad (36)$$

Taking into account (27), we can write

$$\begin{aligned} \dot{V}(\theta) &= -w(t) \int_0^1 f_1(x) \left( \frac{\partial}{\partial x} \left( f_4(x) \frac{\partial \phi}{\partial x} \right) \right)^2 dx \\ &\quad - \sum_{i=1}^3 u_i(t) \int_0^1 g_i(x) \frac{\partial}{\partial x} \left( f_4(x) \frac{\partial \phi}{\partial x} \right) dx \\ &\leq -w(t) f_{1min} \int_0^1 \left( \frac{\partial}{\partial x} \left( f_4(x) \frac{\partial \phi}{\partial x} \right) \right)^2 dx \\ &\quad - \sum_{i=1}^3 u_i(t) \int_0^1 g_i(x) \frac{\partial}{\partial x} \left( f_4(x) \frac{\partial \phi}{\partial x} \right) dx. \end{aligned} \quad (37)$$

Next, we define  $\bar{f} = g_i(x)$  and  $\bar{g} = \frac{\partial}{\partial x} \left( f_4(x) \frac{\partial \phi}{\partial x} \right)$ , and apply *Lemma 1 (Young' inequality)* to (37) in order to obtain

$$\begin{aligned} \dot{V}(\theta) &\leq -w_{min} f_{1min} \int_0^1 \left( \frac{\partial}{\partial x} \left( f_4(x) \frac{\partial \phi}{\partial x} \right) \right)^2 dx \\ &\quad + \sum_{i=1}^3 u_{imax} \left( \frac{1}{2\mu_i} \int_0^1 g_i^2(x) dx + \frac{\mu_i}{2} \int_0^1 \left( \frac{\partial}{\partial x} \left( f_4(x) \frac{\partial \phi}{\partial x} \right) \right)^2 dx \right), \end{aligned}$$

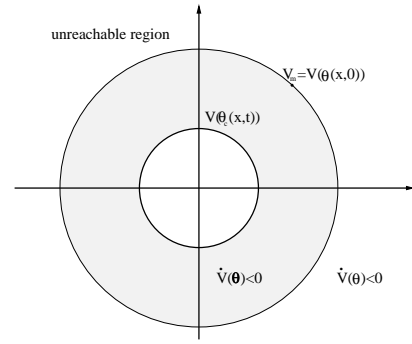


Fig. 3. Diagram of Lyapunov surface when  $V(\theta_c(x, t)) < V(\theta(x, 0))$ .

where  $u_{imax} = \max(u_i(t))$ , ( $i = 1, 2, 3$ ), and we choose  $\mu_i = \frac{w_{min} f_{1min}}{3u_{imax}}$  to attain

$$\begin{aligned} \dot{V}(\theta) &\leq -\frac{w_{min} f_{1min}}{2} \int_0^1 \left( \frac{\partial}{\partial x} \left( f_4(x) \frac{\partial \phi}{\partial x} \right) \right)^2 dx \\ &\quad + \frac{3}{2w_{min} f_{1min}} \sum_{i=1}^3 u_{imax}^2 \int_0^1 g_i^2(x) dx. \end{aligned} \quad (38)$$

By defining  $\tilde{f} = f_4(x) \frac{\partial \phi}{\partial x}$ , we use *Lemma 2 (Dirichlet Poincare' inequality)* to write

$$\begin{aligned} \dot{V}(\theta) &\leq -\frac{w_{min} f_{1min}}{2C} \int_0^1 f_4(x) \theta^2(x, t) dx \\ &\quad + \frac{3}{2w_{min} f_{1min}} \sum_{i=1}^3 u_{imax}^2 \int_0^1 g_i^2(x) dx. \end{aligned} \quad (39)$$

There exists a sufficient large  $\theta_c(x, t)$ , such that

$$\int_0^1 \theta_c^2(x, t) dx = \frac{3C}{w_{min}^2 f_{1min}^2 f_{4min}} \sum_{i=1}^3 u_{imax}^2 G_i, \quad (40)$$

making  $\dot{V}(\theta) \leq 0$ .

Let  $V_m = \max\{V(\theta_c(x, t)), V(\theta(x, 0))\}$ . As shown in Fig. 3, for all  $\theta(x, t)$  outside the Lyapunov surface  $V(\theta_c(x, t))$ , we have  $\dot{V}(\theta(x, t)) < 0$ . This implies that those  $\theta(x, t)$  that are outside the Lyapunov surface  $V_m$  are not reachable (Note that  $V_m$  is a function of the initial condition  $\theta(x, 0)$ ). Consequently, the system is not completely controllable with bounded control inputs.

*Corollary 1:* Assume  $\theta(x, 0) \in C^0(\Omega) \cap L^2(\Omega)$ , then the solution  $\theta(x, t)$  of the system defined by (27)-(33) satisfies

$$V(\theta) = \frac{1}{2} \int_0^1 \theta^2(x, t) dx \leq V_m \quad (41)$$

*Proof:* This is a direct consequence of the fact that  $\dot{V}(\theta(x, t)) < 0$  outside the Lyapunov surface defined by  $V(\theta(x, t)) = V_m$  and  $V(\theta(x, 0)) \leq V_m$  (note definition of  $V_m$ ).

## VI. CONTROLLABILITY OF THE CURRENT PROFILE CONTROL PROBLEM

The poloidal flux system stated in equations (1)-(2) can be written in terms of equations (27)-(32). To simplify the notation, we replace  $\hat{\rho}$  by  $x$  hereafter. We propose first the following homogenization transform,

$$\phi(x, t) = \psi(x, t) - \frac{1}{2} x^2 v(t), \quad (42)$$

which satisfies the homogeneous boundary conditions

$$\begin{aligned}\frac{\partial \phi}{\partial x}(0,t) &= \frac{\partial \psi}{\partial x}(0,t) = 0 \\ \frac{\partial \phi}{\partial x}(1,t) &= \frac{\partial \psi}{\partial x}(1,t) - v(t) = 0.\end{aligned}\quad (43)$$

Then, using (12)-(13) and (42)-(43), it is possible to obtain the following PDE system for  $\phi$ ,

$$\begin{cases} \frac{\partial \phi}{\partial t} = f_1(x)w(t)\frac{\partial}{\partial x}\left(f_4(x)\frac{\partial \phi}{\partial x}\right) - \frac{1}{2}x^2\frac{dv}{dt} \\ \quad + f_1(x)\frac{d(xf_4(x))}{dx}w(t)v(t) + f_2(x)u(t), \\ \frac{\partial \phi}{\partial x}(0,t) = \frac{\partial \phi}{\partial x}(1,t) = 0, \\ \phi(x,0) = \psi_0(x) - \frac{1}{2}x^2v(0) \equiv \phi_0(x). \end{cases}\quad (44)$$

By making

$$g_1(x) = -\frac{1}{2}x^2, g_2(x) = f_1(x)\frac{d(xf_4(x))}{dx}, g_3(x) = f_2(x), \quad (45)$$

and

$$u_1(t) = dv/dt, u_2(t) = w(t)v(t), u_3(x) = u(t), \quad (46)$$

we recover (27)-(29).

Taking into account the definition of the rotational transform  $\iota(x,t)$  in (7), which indeed defines the objective of the current profile control problem, we can use definitions (33) and (42) to write

$$\theta(x,t) = \sqrt{f_4(x)}(B_{\phi,o}\rho_b^2 x \iota(x,t) - xv(t)). \quad (47)$$

Letting  $\alpha = B_{\phi,o}\rho_b^2$  and  $h(x) = \alpha x\sqrt{f_4(x)}$ , we can rewrite (47) as

$$\theta(x,t) = h(x)\left(\iota(x,t) - \frac{1}{\alpha}v(t)\right). \quad (48)$$

Using Corollary 1, we can write

$$\int_0^1 h^2(x)\left(\iota(x,t) - \frac{1}{\alpha}v(t)\right)^2 dx \leq 2V_m. \quad (49)$$

Taking into account (30) this equation becomes

$$\alpha^2 f_{4min} \int_0^1 \left(x \iota(x,t) - \frac{x}{\alpha}v(t)\right)^2 dx \leq 2V_m. \quad (50)$$

We divide both sides of (50) by  $\alpha^2 f_{4min}$  to obtain

$$\int_0^1 \left(x \iota(x,t) - \frac{x}{\alpha}v(t)\right)^2 dx \leq \frac{2V_m}{\alpha^2 f_{4min}}. \quad (51)$$

Then, using *Lemma 1 (Young' inequality)* with  $\mu = 2$ , we can write

$$\begin{aligned} & \int_0^1 \left(x \iota(x,t) - \frac{x}{\alpha}v(t)\right)^2 dx \\ & \geq \int_0^1 x^2 \iota^2(x,t) dx - \frac{1}{2} \int_0^1 x^2 \iota^2(x,t) dx - \frac{2}{3\alpha^2} v^2(t) + \frac{1}{3\alpha^2} v^2(t) \\ & = \frac{1}{2} \int_0^1 x^2 \iota^2(x,t) dx - \frac{1}{3\alpha^2} v^2(t). \end{aligned}$$

Substituting this into (51) results in

$$\frac{1}{2} \int_0^1 x^2 \iota^2(x,t) dx \leq \frac{2V_m}{\alpha^2 f_{4min}} + \frac{v_{max}^2}{3\alpha^2}. \quad (52)$$

By defining

$$V(\iota) = \frac{1}{2} \int_0^1 x^2 \iota^2(x,t) dx, \quad (53)$$

and

$$V_l = \frac{2V_m}{\alpha^2 f_{4min}} + \frac{v_{max}^2}{3\alpha^2}, \quad (54)$$

the reachable region of the rotational transform  $\iota(x,t)$  is bounded by the condition

$$V(\iota) \leq V_l. \quad (55)$$

Given a desired  $\iota^*(x,t)$  profile, if  $V(\iota^*)$  is larger than  $V_l$ , we can conclude that such desired profile is unreachable. The region outside the Lyapunov surface defined by  $(V(\iota(x,t)) = V_l)$  cannot be reached by the system. Therefore, the current profile control problem with bounded actuators is not completely controllable.

## VII. UNREACHABLE ZONE STUDY

In order to prevent a waste of time and resources in present tokamaks, given initial conditions and actuator limitations, it is of great interest to have the capability of determining the unreachable region for the current profile evolution not only experimentally but also theoretically. Equations (53)-(55) actually can be used to estimate the unreachable region of the system.

In this section, we illustrate the approach through an example that uses data from the DIII-D tokamak. The constraints for the actuators, total plasma current  $I(t)$ , average density  $\bar{n}(t)$  and total non-inductive power  $P_{tot}(t)$ , are given as follows

$$\begin{cases} 0.5 \times 10^6 \text{ (A)} \leq I(t) \leq 1.19141 \times 10^6 \text{ (A)} \\ |dI(t)/dt| \leq 2 \times 10^6 \text{ (A/s)} \\ I(t=0) = 0.7092 \times 10^6 \text{ (A)}, \end{cases}\quad (56)$$

$$I \times 10^{19} \text{ (A)} \leq \bar{n}(t) \leq 5I \times 10^{19} \text{ (A)}, \quad (57)$$

$$1 \times 10^6 \text{ (W)} \leq P_{tot}(t) \leq 20 \times 10^6 \text{ (W)}. \quad (58)$$

Using (16)-(20) and  $k_3 = 1.0996 \times 10^{-7}$ , we have

$$\begin{aligned} w_{min} &= 1.778 \times 10^{23}, & w_{max} &= 1.18 \times 10^{25}, \\ v_{min} &= 5.498 \times 10^{-2}, & v_{max} &= 1.31 \times 10^{-1}, \\ u_{min} &= 8.40 \times 10^{-4}, & u_{max} &= 6.3 \times 10^{-3}. \end{aligned}\quad (59)$$

Using this result together with equations (31), (46), and (45), we can obtain

$$\begin{aligned} u_{1min} &= 2.19 \times 10^{-1}, & G_1 &= 5 \times 10^{-2}, \\ u_{2min} &= 1.46 \times 10^{24}, & G_2 &= 8.9 \times 10^{-39}, \\ u_{3min} &= 6.3 \times 10^{-3}, & G_3 &= 20.4112. \end{aligned}\quad (60)$$

According to equations (15), (21) and (71), we can write

$$f_{1min} = 6.7 \times 10^{-18}, f_{4min} = 1.8, C = 1. \quad (61)$$

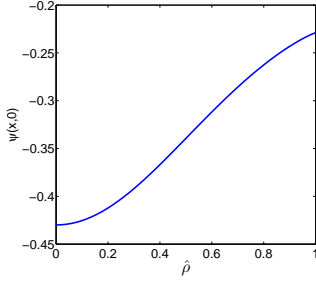


Fig. 4. Initial  $\psi$ .

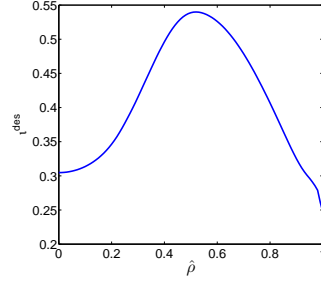


Fig. 5. Desired  $\iota$  profile.

By inserting these values in (40) we obtain

$$V(\theta_c(x,t)) = 0.0224. \quad (62)$$

Let us consider an initial flux profile  $\psi(x,0)$  extracted from experimental shot 119556 in DIII-D and shown in Fig. 4. Let us also consider the desired  $\iota$  profile shown in Fig. 5. Taking into account that  $v(t=0) = 0.0779$ , we use equations (33) and (44) to obtain  $\theta(x,0)$ , and then

$$V(\theta(x,0)) = 0.0229. \quad (63)$$

Since  $V(\theta_c(x,t)) < V(\theta(x,0))$ , we adopt  $V_m = V(\theta(x,0))$ . Taking into account that  $\alpha = 1.1546$ , we use (54) to finally achieve

$$V_l = 0.0234. \quad (64)$$

We compute (53) for the desired  $\iota$  profile to obtain

$$V(\iota^{des}) = 0.0288. \quad (65)$$

Since  $V_l < V(\iota^{des})$ , we can conclude that the desired profile  $\iota^{des}$  is not reachable for the given initial condition and actuator constraints.

## VIII. CONCLUSIONS AND FUTURE WORKS

This paper represents the first attempt to study the controllability of the current profile system in tokamak plasmas. The poloidal flux profile evolution is modeled by a parabolic PDE system with bounded actuators. We prove that the system is not completely controllable and we provide an estimate for the unreachable region.

This just initiated research effort is far from being finished. The results presented in this paper provide only an estimate for the unreachable region, which is in addition quite conservative. The definition of a reachable region, although more challenging, is probably of more interest. To achieve this goal the controllability analysis will need to be carried out over a finite-time horizon, since the reachable region in this case may be much smaller than in the infinite-time horizon case. Future work will also focus on reducing the conservatism in the reachable region estimate. For instance, the effect on controllability of the spatial distribution of the control action (given by the  $g_i(x)$ 's terms) needs to be better accounted for. Two control inputs with the same power but different spatial distributions can impact the size and shape of the reachable zone in very different ways.

This work aims at preventing fusion experimentalists from wasting enormous amounts of effort and time attempting

to achieve current profiles that are indeed unreachable for the given initial conditions and actuator constraints. Recommendations in terms of the control action distribution, i.e. actuator design, arising from the controllability analysis may be of enormous importance for the upgrade of present tokamaks and the construction of new ones.

## APPENDIX

Since the problem is 1-D, we will prove Lemma 2 for the case  $n = 1$ . Let  $U : [a, b]$ ,  $r = b - a$  and  $f' = \frac{df}{dx}$ . The statement becomes

$$\int_a^b f^2 dx \leq kr^2 \int_a^b (f')^2 dx, \quad (66)$$

where  $f$  is a  $C^1$  function satisfying  $f(a) = f(b) = 0$ . By the Fundamental Theorem of Calculus we know that

$$f(s) = f(s) - f(a) = \int_a^s f'(x) dx \quad (67)$$

Therefore,

$$|f(s)| \leq \int_a^s |f'(x)| dx. \quad (68)$$

We apply the Cauchy-Schwarz inequality

$$\int hg dx \leq \left( \int h^2 dx \right)^{1/2} \left( \int g^2 dx \right)^{1/2}, \quad (69)$$

with  $h = 1$ ,  $g = |f'|$  to obtain

$$|f(s)| \leq \sqrt{\int_a^s (f')^2 dx} \sqrt{s-a} \leq \sqrt{\int_a^b (f')^2 dx} \sqrt{b-a}.$$

Squaring both sides gives

$$|f(s)|^2 \leq r \int_a^b (f'(s))^2 ds. \quad (70)$$

We finally integrate over  $[a, b]$  to obtain

$$\int_a^b f^2(s) ds \leq r^2 \int_a^b (f'(s))^2 ds, \quad (71)$$

as required ( $k = 1$ ).

## REFERENCES

- [1] J. C. Hsu and A. V. Meyer, *Modern Control Principles and Application*. McGraw-Hill, New York, 1968.
- [2] E. B. Lee and L. Markus, *Foundations of Optimal Control Theory*. Wiley, New York, 1967.
- [3] W. Liu and G. H. Williams, "Exact Neumann boundary controllability for problems of transmission of the wave equation," *Glasgow Math. J.*, vol. 41, pp. 125–139, 1999.
- [4] S. Bezerra and D. Menezes, "Approximate controllability for the semi-linear heat equation in  $R^N$  involving gradient terms," *Computational and Applied Mathematics*, vol. 22, no. 1, p. 123C148, 2003.
- [5] P. Lin, H. gao, and X. Liu, "Some results on controllability of a nonlinear degenerate parabolic systems by bilinear control," *Journal of Mathematical Analysis and Applications*, pp. 1149–1160, 2007.
- [6] R. Mohler, *Bilinear Control Processes with Application to Engineering, Ecology, and Medicine*. Academic Press, New York and London, 1973.
- [7] Y. Ou, T. Luce, E. Schuster, *et al.*, "Towards model-based current profile control at DIII-D," *Fusion Engineering and Design*, vol. 82, pp. 11153–1160, 2007.
- [8] J. Wesson, *Tokamaks*, 3rd ed. Clarendon Press, Oxford, 2004.
- [9] L. C. Evans, *Partial Differential Equations (Graduate Studies in Mathematics, V. 19)*. New York: American Mathematical Society, 1998.